THE ASTROPHYSICAL JOURNAL, 354:438–445, 1990 May 10

THE DWARF SPHEROIDAL GALAXY ANDROMEDA I

JEREMY MOULD
Palomar Observatory, California Institute of Technology
AND
JEROME KRISTIAN
Observatories of the Carnegie Institution of Washington
Received 1989 August 24; accepted 1989 November 6

ABSTRACT

Images of Andromeda I in the visual and near-infrared show a giant branch characteristic of Galactic globular clusters of intermediate metallicity. The distance of the galaxy is estimated from the tip of the giant branch to be 790 ± 60 kpc. The physical dimensions and luminosity are similar to those of the dwarf spheroidal in Sculptor. There is no evidence for an intermediate age population in Andromeda I, and appropriate upper limits are specified. There is marginal evidence for a color gradient in the galaxy, a phenomenon not previously noted in a dwarf spheroidal.

Subject headings: galaxies: distances — galaxies: individual (And I) — galaxies: Local Group — galaxies: photometry — galaxies: stellar content

I. INTRODUCTION

The dwarf spheroidal companions of the Milky Way have an interesting dual character. On the one hand, galaxies such as Ursa Minor have color-magnitude diagrams almost indistinguishable from those of globular clusters. On the other, there are systems like Carina in which there is a considerable population of intermediate age (Mould and Aaronson 1983; Mateo and Nemec 1989; Mighell 1989). The other five dwarf spheroidals are a blend of these characteristics—some more like Ursa Minor, others more like Carina (Da Costa 1988).

There are so few of these objects to study, and yet their importance at the faint end of the elliptical galaxy luminosity function is so great, that it seems necessary to turn to our neighbor in the Local Group, M31, to learn more about this class. In this paper we present a color-magnitude diagram of Andromeda I, a dwarf spheroidal discovered in M31 by van den Bergh (1971) on Palomar Schmidt IIIa-J plates.

II. PHOTOMETRY

CCD images of And I were obtained on 1983 October 30 (UT) at the prime focus of the Hale Telescope. Details are given by Mould and Kristian (1986, hereafter MK86). We obtained nine 300 s exposures in I but were able to secure only two 450 s exposures in V, before poor seeing, followed by fog, intervened. Image processing and calibration of the photometry on the Cousins system are described by MK86. Figure 1 (Plate 23) shows the stacked V frame, in which the concentration of faint images toward the center of the picture is Andromeda I. Examination of this frame and comparison with R. Racine's Schmidt plate (van den Bergh 1971) indicates the center of And I is approximately located at (300, 300), and the radius of the dwarf is approximately 300 pixels (2′). The dimensions of the frame are 800 × 800 pixels.

Both the V and I frames were searched for images with the DAOPHOT program (Stetson 1987). Photometry was carried out by point-spread function fitting. Those images with $I < 23$ were used for the construction of color-magnitude diagrams. The density of these images as a function of radius r is shown in Figure 2, where r is the radial distance in pixels from (300, 300). On the basis of this density distribution, we have segregated the images into a "dwarf" sample ($0 < r < 300$) and a "field" sample ($300 < r < 500$). These samples are of equal area on the chip and avoid the poorly flattened regions at the corners of the chip. And I is 3°.3 from the center of M31. At even half that galactocentric distance, M31 halo stars are a minor contributor to the observed star density (see Mould 1986, Fig. 7). We therefore expect a negligible contribution from the halo of M31 to these fields. The main usefulness of the "field" sample is thus accurate statistical cancellation of the Galactic foreground and distant background from the "dwarf" sample.

Photometry of stars with $I < 22$ is recorded in Table 1 for the dwarf sample and Table 2 for the field sample. The finding charts in Figures 3*a* and 3*b* (Plates 24–25) are made from the I frame of And I. There is a systematic uncertainty of ± 0.03 mag in the zeropoint of each of V and I, which comes about when transforming from point-spread function scaling ratios to total fluxes. Random errors were estimated by the insertion of artificial stars in the V frame. The rms error is 0.07 mag at $V = 22$, rising to 0.3 mag at $V = 23$. The later is 2–3 times larger than photon statistics would predict and is a result of image crowding. Uncertainties in the colors are discussed in § V.

III. COLOR-MAGNITUDE DIAGRAMS

Figure 4 is a color-magnitude diagram of the dwarf sample for all stars with $I < 23$. The red giant branch of And I is clearly visible starting at $I \approx 20.5$. The giant branch tip is at approximately the same magnitude in And I as in the M31 halo field observed by MK86. The M31 giant branch extended to much redder colors, however. Figure 5 is the corresponding plot of the field sample. A sparse giant branch is still visible, because Andromeda I spills over into the "field" sample (see Fig. 2).

A useful way of displaying the difference between these two samples is to subtract a star from the first sample wherever a star in the second sample occurs in close proximity in the C-M diagram. Figure 6 was constructed in this way [defining proximity to be $\delta I \leq 0.2$, $\delta(V-I) \leq 0.1$]. It shows filled symbols for uncanceled stars and open ones for excess field stars. The M92 and 47 Tuc giant branches (Mould, Kristian, and Da Costa

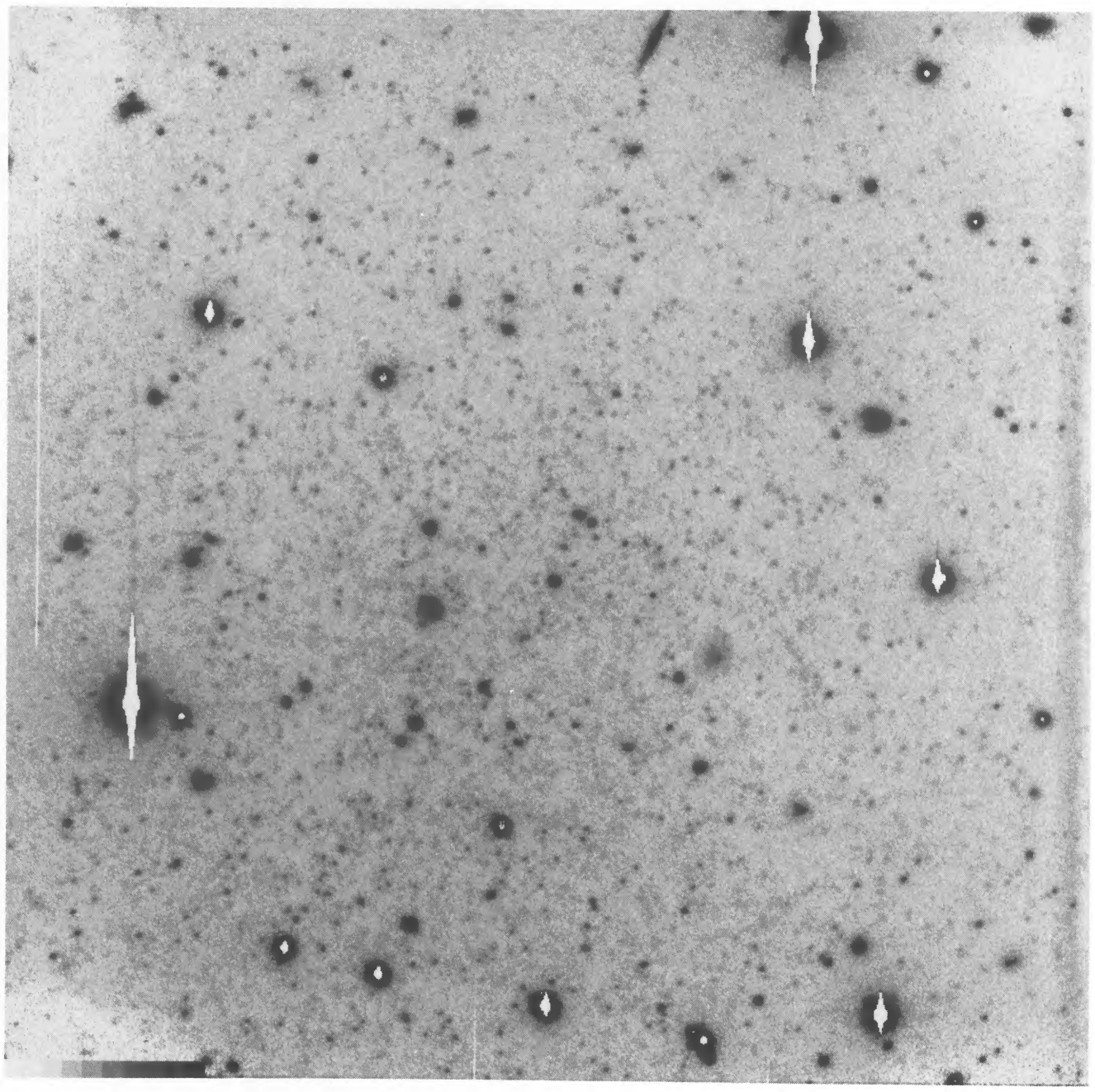

FIG. 1.—The galaxy Andromeda I in the V bandpass. The scale is 0.″42 pixel^{-1}. North is down, and east is to the right. Total exposure time is 2700 s; the limiting magnitude is $V \sim 25$.

MOULD AND KRISTIAN (*see* **354**, 438)

PLATE 24

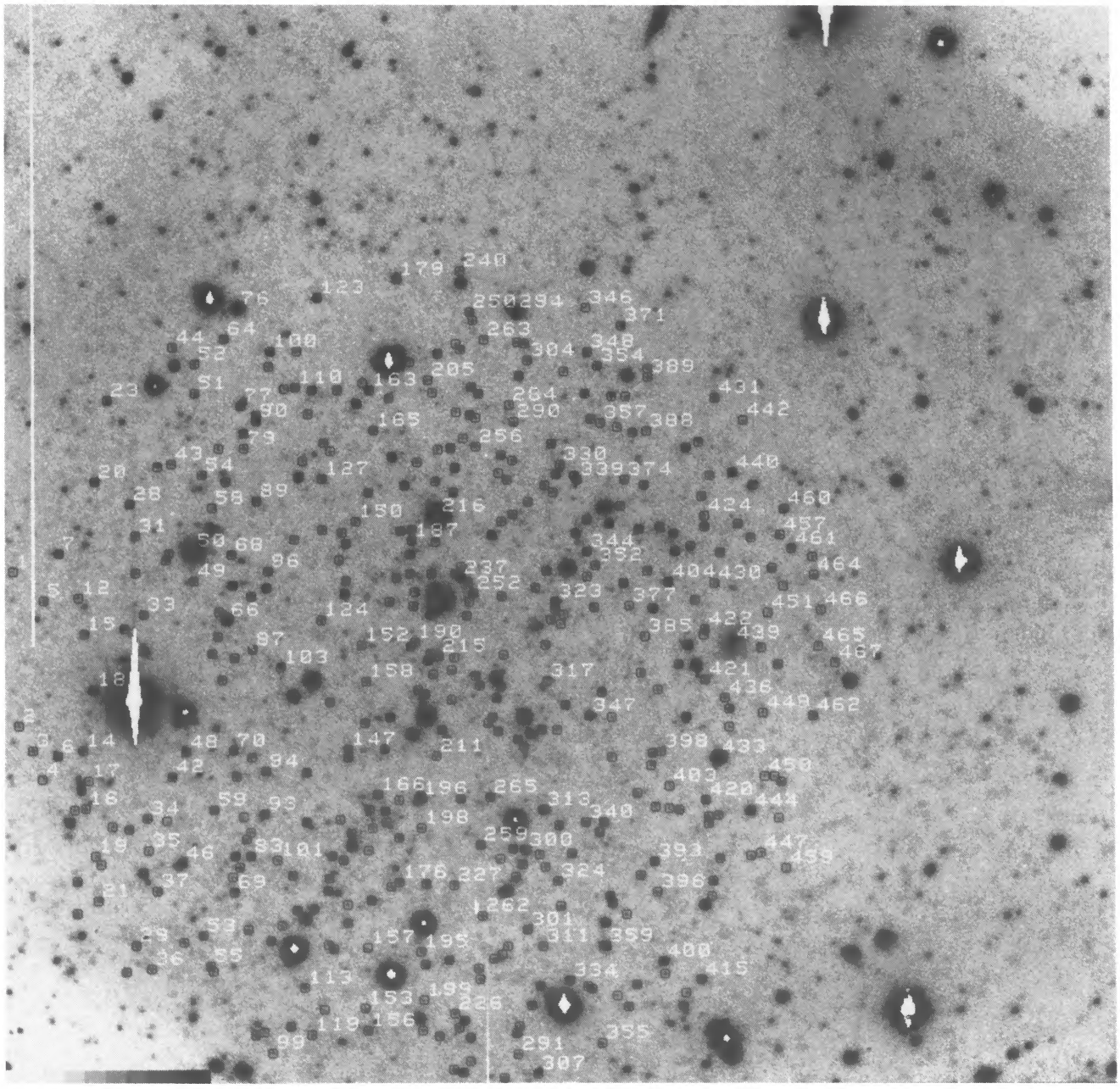

FIG. 3*a*

FIG. 3.—(*a*) The galaxy Andromeda I in the *I* bandpass. The scale is 0.″42 pixel^{-1}. North is down, and east is to the right. The numbered stars represent the "dwarf" sample. All stars in Table 1 are circled. To avoid confusion, only some stars are labeled with numbers. In each case the number appears in the same position, just above and to the right of the corresponding star image. Unlabeled stars can be located by interpolation, using the *x*-*y* coordinates in Table 1. (*b*) The galaxy Andromeda I in the *I* bandpass. The scale and orientation are the same as Fig. 1. The numbered stars represent the "field" sample and refer to Table 2.

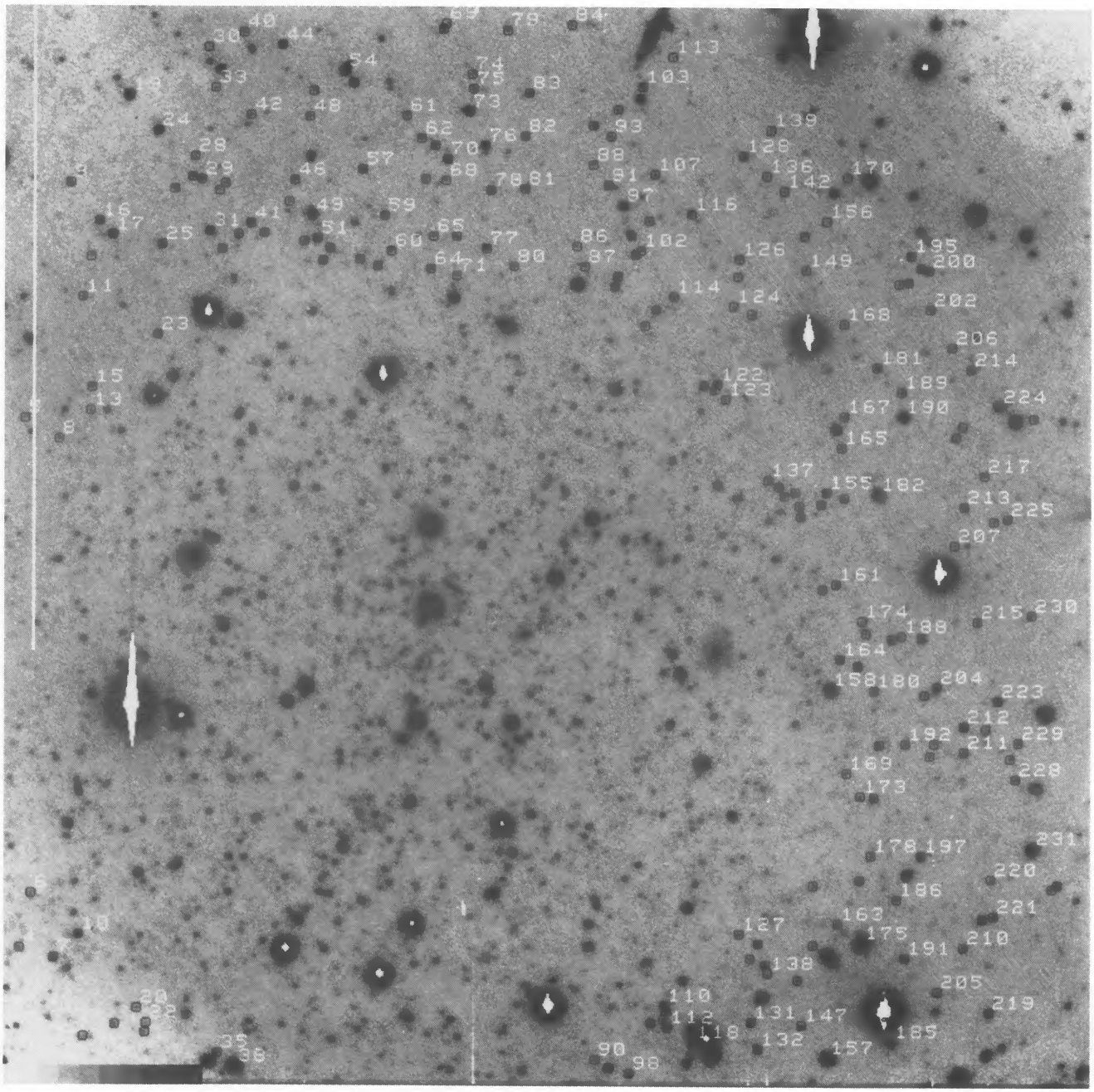

FIG. 3*b*

MOULD AND KRISTIAN (*see* **354**, 438)

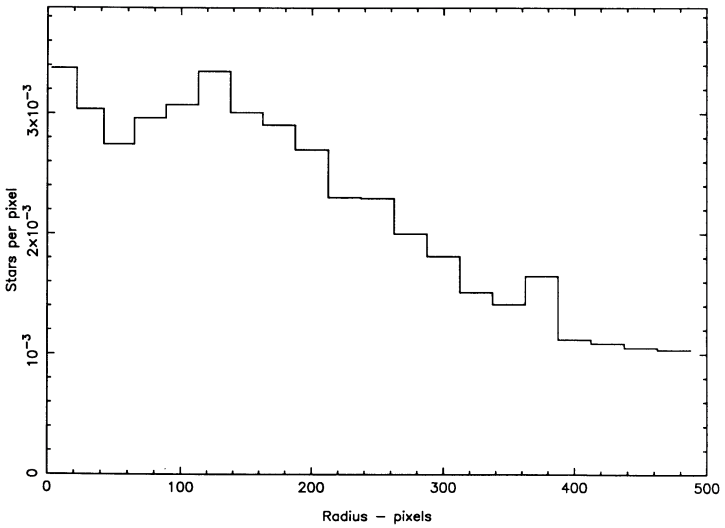

FIG. 2.—Radial profile of the star density. The scale is 0".42 pixel^{-1}. The adopted magnitude limit is $I = 23$.

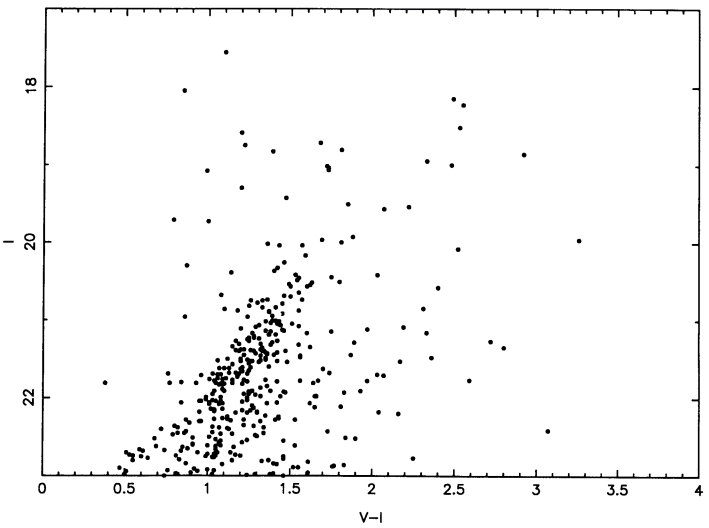

FIG. 5.—Color-magnitude diagram for the "field" sample in Fig. 3*b* and Table 2.

1983) have been superposed at $(m-M)_I = 24.45$ and $E(V-I) = 0.04$. Galactic extinction of $E(B-V) = 0.03$ mag has been adopted based on the Burstein and Heiles (1982) 21 cm map of the region. The distance modulus $(m-M)_0 = 24.4$ is that of MK86 for M31.

With two small qualifications discussed below, we can say that the giant branch of And I is contained by the globular cluster giant branches and seems to prefer the low-metallicity, blue side of the boundary. There is no apparent excess of "dwarf" over "field" for $I < 20$, and the spread in color that is apparent for $I > 22$ does not exceed the estimated errors. There are about 20 stars bluer than M92 at $I = 21$; these could be asymptotic giant branch stars of M92 composition. There are a few stars brighter than the giant branch tip of M92 with $1.6 < V-I < 1.9$; these could be long-period variables like those seen in globular clusters (Frogel and Elias 1988). In brief, the giant branch of And I looks like a simple Population II giant branch. We proceed to a more quantitative examination in § V.

IV. THE LUMINOSITY FUNCTION AND DISTANCE MODULUS

Binning and subtracting the I band photometry for the two samples, we obtain the luminosity function plotted in Figure 7. The tip of the giant branch is at $I = 20.55 \pm 0.05$. The mean value of $V-I$ at this location is 1.5, and hence m_{bol} at the tip is 21.05 ± 0.1 (Mould, Kristian, and Da Costa 1984). (We have supposed a reddening uncertainty as large as the reddening itself.) Equation (4) of Frogel, Cohen, and Persson (1983) predicts $M_{bol} = -3.45 \pm 0.1$ and is based on a Population II distance scale for which $M_V = 0.6$ for metal-poor RR Lyraes and $M_V = 0.8$ for metal-rich ones. The distance modulus of And I on this scale is therefore $(m-M)_0 = 24.5 \pm 0.15$. This result is in close agreement with the distance of M31 on the same scale (MK86).

V. THE GIANT BRANCH

Figure 8 shows the distribution of colors for $21.45 < I < 21.65$ (i.e., at $M_I = -3$) in the dwarf sample. For 69 stars

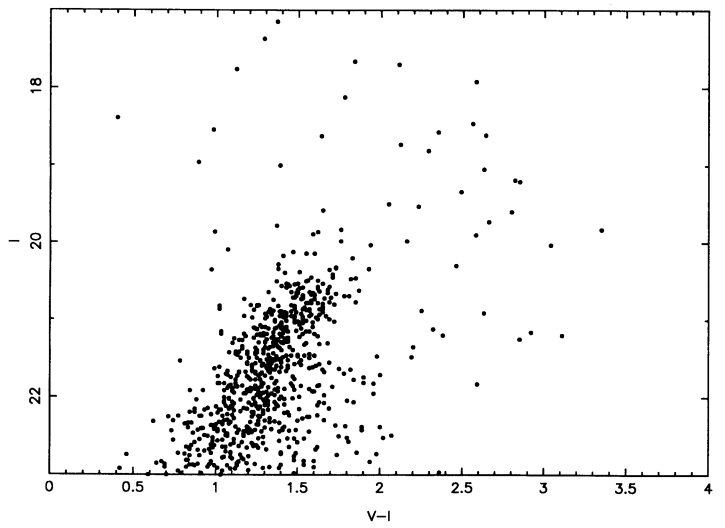

FIG. 4.—Color-magnitude diagram for the "dwarf" sample in Fig. 3*a* and Table 1.

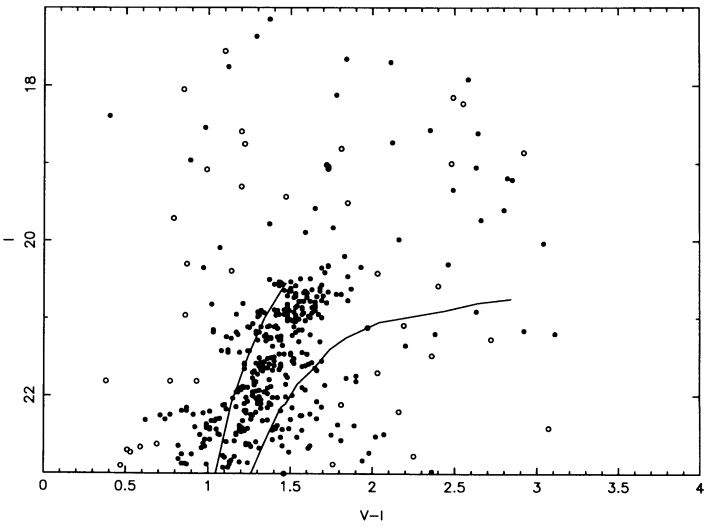

FIG. 6.—Field-subtracted color-magnitude diagram. The solid lines indicate the giant branches of M92 (*left*) and 47 Tuc (*right*) shifted by the appropriate relative distance modulus and reddening.

TABLE 1

PHOTOMETRY FOR THE ANDROMEDA I DWARF SAMPLE

#	x	y	I	V − I	#	x	y	I	V − I	#	x	y	I	V − I	#	x	y	I	V − I
1	10	374	21.87	1.32	60	157	327	21.14	1.49	119	223	40	21.55	1.19	178	286	209	21.82	1.46
2	14	263	21.69	1.24	61	158	345	21.70	1.27	120	225	131	20.50	1.55	179	286	585	20.64	1.32
3	24	245	21.47	1.98	62	158	463	21.77	1.12	121	225	296	17.66	1.84	180	288	403	21.12	2.32
4	31	224	21.71	2.00	63	160	296	21.31	1.63	122	225	505	20.49	1.56	181	291	436	20.71	1.47
5	32	353	21.46	1.60	64	162	542	20.91	1.41	123	229	572	20.33	1.73	182	295	257	18.96	0.89
6	42	241	20.78	1.62	65	163	439	20.95	1.43	124	231	339	21.52	1.33	183	295	320	21.52	1.36
7	43	387	20.41	1.71	66	164	339	18.61	2.64	125	232	58	21.88	1.38	184	295	372	21.57	1.48
8	51	193	19.00	1.39	67	167	154	21.99	1.51	126	232	404	21.66	1.07	185	295	386	20.67	1.58
9	54	202	21.76	1.48	68	167	386	20.95	1.46	127	232	441	20.73	1.52	186	295	525	21.67	1.66
10	56	128	20.86	1.33	69	168	143	20.45	1.58	128	233	467	21.32	1.37	187	296	396	21.03	1.51
11	56	151	20.69	1.81	70	168	245	20.84	1.54	129	235	105	21.51	1.31	188	296	404	21.26	1.38
12	57	355	21.69	1.78	71	168	364	20.49	1.62	130	235	144	20.68	1.60	189	297	349	21.39	1.40
13	59	216	20.65	1.68	72	169	169	20.32	1.73	131	236	153	20.99	1.62	190	298	323	21.50	1.40
14	60	245	21.04	1.52	73	169	312	21.15	1.57	132	237	280	21.52	1.27	191	298	359	21.72	1.30
15	61	329	20.57	1.69	74	170	226	21.20	3.11	133	238	169	20.90	1.42	192	300	52	19.89	1.59
16	62	203	21.44	1.24	75	172	161	21.21	1.62	134	238	461	21.84	1.28	193	300	289	21.25	1.38
17	64	223	21.77	1.84	76	172	564	18.57	2.35	135	239	102	20.53	1.50	194	300	453	21.56	1.24
18	68	289	19.21	2.85	77	174	494	20.64	1.57	136	243	505	21.10	1.23	195	301	100	21.85	1.24
19	69	169	21.64	1.82	78	175	197	21.67	1.14	137	244	195	21.82	1.29	196	301	210	19.34	2.49
20	69	439	20.53	1.65	79	176	463	21.64	1.36	138	244	382	21.60	1.31	197	302	43	21.77	1.24
21	71	137	21.09	1.43	80	176	474	20.59	1.51	139	246	166	20.87	1.55	198	302	189	21.88	1.21
22	73	163	21.60	1.33	81	177	181	21.28	1.30	140	246	402	21.55	1.40	199	303	65	21.95	1.18
23	78	498	20.69	1.78	82	178	116	21.44	1.57	141	248	358	20.35	1.69	200	304	91	20.82	1.25
24	81	190	21.67	1.39	83	180	169	20.54	1.48	142	249	121	21.00	1.36	201	305	149	21.18	1.60
25	90	333	20.96	1.53	84	180	186	21.67	1.24	143	249	134	21.92	1.59	202	305	286	20.93	1.63
26	91	86	21.20	2.38	85	181	240	21.58	1.29	144	249	367	21.23	1.34	203	306	270	17.15	1.37
27	93	188	20.95	1.48	86	181	356	20.86	1.65	145	249	394	20.86	1.53	204	307	310	20.73	1.60
28	94	423	20.71	1.70	87	182	318	20.72	1.53	146	250	240	20.96	1.31	205	308	512	21.82	1.36
29	98	105	21.35	2.20	88	183	40	21.25	1.37	147	250	246	20.75	1.58	206	309	315	21.32	1.54
30	98	373	21.70	1.06	89	185	425	20.92	1.52	148	252	176	19.53	2.23	207	309	343	20.34	1.38
31	98	400	21.30	1.55	90	185	483	20.64	1.50	149	252	185	20.91	2.63	208	310	372	21.11	1.32
32	103	157	19.19	2.82	91	185	487	21.11	1.32	150	256	410	21.72	1.26	209	311	300	21.66	1.43
33	104	343	21.16	2.92	92	189	42	21.62	1.57	151	257	495	20.88	2.25	210	311	503	21.77	1.21
34	106	196	21.11	1.40	93	190	199	20.71	1.48	152	260	321	21.94	1.29	211	313	241	21.85	1.16
35	107	173	21.84	1.63	94	191	230	20.66	1.73	153	261	59	21.57	1.32	212	313	395	21.66	1.22
36	109	88	21.45	1.50	95	192	362	20.09	1.07	154	261	510	21.92	1.60	213	313	439	21.09	1.30
37	113	144	21.24	1.42	96	193	374	20.86	1.63	155	262	265	21.52	1.52	214	314	39	21.17	1.29
38	114	450	21.30	1.68	97	194	108	20.81	1.46	156	263	43	20.98	1.30	215	315	313	21.82	1.01
39	120	194	21.94	1.29	98	194	522	21.46	1.43	157	263	103	21.89	1.42	216	315	414	16.55	1.71
40	120	382	20.97	1.61	99	195	27	21.72	1.13	158	263	295	21.59	1.61	217	315	462	21.91	1.05
41	122	387	21.50	1.40	100	195	533	20.63	1.63	159	264	173	21.85	1.52	218	315	531	20.54	1.44
42	124	226	20.95	1.57	101	199	166	21.62	1.33	160	265	202	21.50	1.33	219	316	354	16.50	1.51
43	124	452	21.55	1.51	102	202	119	21.60	1.22	161	265	431	21.09	1.59	220	317	260	20.57	1.62
44	125	536	21.46	1.46	103	202	305	21.02	1.72	162	266	137	20.35	0.97	221	321	94	20.65	1.50
45	127	523	18.73	2.12	104	205	506	21.89	1.10	163	266	505	20.65	1.49	222	324	15	21.49	1.20
46	131	164	19.83	1.76	105	208	46	21.02	1.36	164	267	189	21.82	1.12	223	324	282	21.91	0.92
47	132	107	21.42	1.25	106	210	155	21.27	1.36	165	269	476	21.38	1.29	224	324	303	21.97	1.25
48	134	244	20.79	1.65	107	211	285	18.54	0.98	166	271	213	21.26	1.16	225	324	463	21.09	1.28
49	140	367	21.17	1.41	108	212	397	21.46	1.54	167	276	201	20.88	1.35	226	325	55	21.34	1.16
50	140	389	18.12	1.78	109	213	130	21.01	1.43	168	276	246	20.88	1.57	227	325	148	21.49	1.33
51	141	503	21.41	1.14	110	213	507	21.03	1.59	169	277	193	21.58	1.52	228	326	312	21.94	1.11
52	141	524	21.35	1.30	111	214	533	21.35	1.45	170	280	147	21.56	1.32	229	326	431	21.01	1.48
53	146	112	20.82	1.38	112	215	442	19.90	2.58	171	280	269	20.61	1.50	230	327	372	21.18	1.53
54	146	444	21.28	1.43	113	218	74	21.16	1.35	172	280	352	21.35	1.38	231	327	449	20.30	2.46
55	151	90	21.25	2.85	114	218	454	21.53	1.27	173	280	499	21.45	1.50	232	328	45	21.39	1.25
56	153	86	21.85	1.47	115	219	124	19.05	2.63	174	282	457	20.58	1.53	233	328	489	21.90	1.19
57	153	315	21.22	1.51	116	220	193	20.77	1.69	175	285	369	21.04	1.53	234	328	538	21.85	1.62
58	153	420	21.73	1.47	117	220	229	20.97	1.22	176	286	150	20.80	1.72	235	330	210	21.11	1.24
59	154	202	20.82	1.48	118	222	488	21.60	1.37	177	286	182	21.03	1.40	236	331	13	20.61	1.68

TABLE 1—*Continued*

#	x	y	I	V − I	#	x	y	I	V − I	#	x	y	I	V − I	#	x	y	I	V − I
237	331	369	20.83	1.65	295	372	539	21.74	1.90	353	429	186	20.92	1.30	411	492	463	20.69	1.53
238	331	377	21.93	1.31	296	373	515	20.90	1.49	354	429	522	21.07	1.27	412	493	321	19.60	2.80
239	331	534	21.18	1.31	297	374	163	21.05	1.40	355	430	34	21.64	1.34	413	495	392	21.21	1.18
240	331	591	21.67	1.18	298	375	248	21.06	1.51	356	431	287	20.95	1.48	414	498	353	21.34	1.35
241	332	50	20.47	1.82	299	375	269	17.92	2.58	357	431	481	21.83	2.59	415	501	80	19.73	2.66
242	332	582	18.39	0.40	300	376	173	19.83	3.35	358	432	193	20.90	1.32	416	501	467	21.11	1.43
243	333	470	21.95	1.17	301	377	116	21.37	1.16	359	433	104	20.03	1.94	417	503	428	21.44	1.12
244	335	342	21.30	1.41	302	377	538	21.18	1.39	360	433	121	19.98	1.76	418	504	134	18.81	2.29
245	336	21	21.82	1.96	303	379	424	21.42	1.08	361	434	420	17.70	2.11	419	504	328	21.89	1.57
246	336	38	20.89	1.39	304	379	526	21.18	1.17	362	436	140	20.14	1.55	420	505	209	20.93	1.58
247	336	366	20.99	1.69	305	380	61	20.81	1.26	363	437	408	20.14	1.60	421	505	296	21.36	1.39
248	337	352	21.74	1.09	306	380	257	20.28	1.38	364	438	135	20.64	1.46	422	505	332	21.64	1.65
249	338	487	21.07	1.39	307	384	12	20.72	1.66	365	438	240	21.59	1.44	423	505	406	21.20	1.27
250	338	561	21.15	1.44	308	384	362	21.51	1.38	366	438	269	21.95	1.28	424	505	414	21.61	1.40
251	339	507	20.81	1.21	309	386	75	20.34	1.93	367	439	500	21.18	1.03	425	507	192	21.45	1.32
252	340	358	21.39	1.47	310	386	170	21.30	1.10	368	441	68	21.92	1.21	426	507	197	21.45	1.13
253	340	555	21.62	1.31	311	388	104	21.29	1.30	369	443	478	21.92	1.38	427	509	140	21.93	1.26
254	341	299	21.29	1.35	312	388	260	20.46	1.85	370	445	421	21.02	1.50	428	509	443	21.53	0.78
255	342	88	21.24	1.44	313	389	202	20.03	3.04	371	446	551	21.20	1.28	429	510	151	20.67	1.58
256	342	464	21.43	1.29	314	390	161	21.51	1.35	372	447	365	20.56	1.45	430	512	365	21.84	1.09
257	342	485	21.86	1.28	315	391	321	21.71	1.07	373	448	127	21.68	1.14	431	513	499	21.10	1.41
258	343	80	21.63	1.75	316	391	436	21.42	1.24	374	448	440	21.56	1.34	432	514	198	21.25	1.31
259	344	177	20.62	1.87	317	392	295	21.89	1.22	375	449	60	21.21	1.40	433	514	240	17.76	1.12
260	344	292	20.78	1.58	318	392	374	20.78	1.56	376	449	500	21.61	1.22	434	515	167	20.97	1.48
261	344	502	21.03	1.48	319	395	339	21.43	1.35	377	451	349	21.98	1.32	435	516	387	21.13	1.42
262	345	126	21.49	1.57	320	396	466	20.93	1.34	378	451	515	18.46	2.56	436	519	283	21.29	1.40
263	348	541	21.72	1.30	321	397	431	21.66	1.32	379	454	474	20.91	1.43	437	522	262	21.95	1.27
264	350	265	21.77	1.27	322	398	347	21.44	1.19	380	455	76	21.02	1.49	438	522	275	20.95	1.17
265	351	211	20.90	1.65	323	398	352	20.97	1.42	381	456	214	21.37	1.32	439	525	322	20.86	1.02
266	353	95	21.39	1.29	324	399	151	21.10	1.37	382	458	155	20.68	1.53	440	525	445	19.98	2.16
267	353	269	21.19	1.25	325	399	260	21.67	1.39	383	458	404	20.12	1.47	441	529	408	21.29	1.26
268	353	400	19.78	1.37	326	399	444	20.45	1.71	384	459	301	21.52	1.44	442	533	483	21.95	1.96
269	356	283	20.65	1.59	327	400	191	20.85	1.48	385	462	327	21.97	1.66	443	537	169	21.49	1.25
270	356	298	19.86	0.99	328	401	133	21.35	1.33	386	462	436	21.15	1.55	444	537	201	19.50	2.05
271	357	259	20.73	1.17	329	402	336	21.90	1.48	387	464	374	21.57	1.29	445	538	398	21.23	1.23
272	358	167	21.90	1.36	330	402	451	21.57	1.19	388	464	475	21.94	1.26	446	540	436	20.50	1.37
273	358	445	21.88	1.07	331	404	343	21.61	1.22	389	465	514	21.47	1.37	447	544	171	21.47	1.50
274	359	98	21.58	1.22	332	405	278	20.69	1.49	390	465	520	21.55	1.69	448	545	319	21.48	2.19
275	359	291	20.53	1.43	333	405	518	21.88	1.26	391	466	234	21.28	1.43	449	546	272	21.92	1.19
276	360	9	21.21	1.35	334	407	79	20.58	1.43	392	467	243	21.36	1.24	450	547	226	21.82	1.05
277	360	356	21.68	1.24	335	407	376	17.37	1.29	393	468	165	20.59	1.62	451	550	344	21.99	1.27
278	360	410	21.59	1.37	336	409	171	20.96	1.41	394	468	347	20.20	1.83	452	553	376	21.49	1.15
279	360	458	21.11	1.52	337	412	443	21.15	1.03	395	469	204	21.86	1.13	453	554	226	21.81	1.90
280	361	314	21.92	1.20	338	413	401	20.82	1.02	396	470	143	21.57	1.63	454	557	196	21.82	1.02
281	362	144	19.58	1.65	339	414	440	20.95	1.39	397	471	289	21.68	1.28	455	557	307	21.20	1.29
282	363	104	21.73	1.01	340	419	193	21.28	1.44	398	473	244	21.65	1.22	456	559	222	21.24	1.11
283	364	440	21.48	1.41	341	420	75	21.62	1.44	399	473	406	20.56	1.40	457	559	400	21.68	1.33
284	366	494	21.86	1.71	342	420	502	20.95	1.67	400	474	93	20.38	1.51	458	561	363	21.97	1.36
285	367	174	20.98	1.53	343	421	370	21.81	1.28	401	475	84	21.75	1.20	459	562	160	21.89	1.24
286	368	415	20.90	1.49	344	421	388	20.74	1.35	402	479	203	21.91	0.84	460	562	419	21.26	1.14
287	368	454	21.73	1.19	345	421	411	21.01	1.55	403	479	219	21.95	1.34	461	567	390	20.78	1.55
288	369	41	20.67	1.60	346	421	564	21.99	1.40	404	479	366	20.17	1.41	462	582	270	20.89	1.40
289	369	154	21.18	1.27	347	422	270	20.39	1.42	405	483	401	20.81	1.25	463	582	384	21.75	1.34
290	369	482	21.86	1.12	348	422	532	20.86	1.57	406	484	388	21.41	1.12	464	583	371	21.79	1.37
291	370	26	21.61	1.02	349	423	73	21.23	1.44	407	486	202	21.11	1.36	465	586	320	21.59	1.28
292	371	46	21.61	1.59	350	424	484	21.12	1.25	408	486	307	20.87	1.23	466	588	346	21.92	1.10
293	371	253	20.77	1.85	351	426	348	20.89	1.46	409	490	70	21.85	1.08	467	598	308	21.63	0.99
294	371	561	18.62	1.64	352	427	378	21.41	1.19	410	491	269	19.86	1.62					

TABLE 2

PHOTOMETRY FOR THE ANDROMEDA I FIELD SAMPLE

#	x	y	I	V − I	#	x	y	I	V − I	#	x	y	I	V − I	#	x	y	I	V − I
1	8	90	21.75	1.11	60	286	617	21.38	1.20	119	515	518	21.07	1.31	177	636	669	18.05	0.85
2	8	226	21.51	1.35	61	297	717	21.77	1.35	120	523	25	17.56	1.10	178	638	172	21.78	1.04
3	9	176	21.06	1.43	62	308	700	21.13	1.45	121	523	515	21.32	1.38	179	640	215	20.88	1.55
4	16	102	21.32	1.55	63	311	670	21.52	1.32	122	525	519	21.02	1.43	180	640	294	21.39	1.17
5	18	492	21.82	1.10	64	315	604	21.01	1.41	123	531	508	21.69	1.19	181	642	532	20.85	2.31
6	24	142	21.62	1.13	65	317	628	21.66	1.21	124	537	577	21.91	1.04	182	643	439	18.95	2.33
7	41	95	20.37	1.40	66	318	695	21.02	1.35	125	540	599	21.69	1.03	183	644	254	21.04	1.38
8	43	477	21.96	1.29	67	324	781	21.56	1.25	126	541	612	21.46	1.32	184	653	332	20.82	1.25
9	51	666	21.14	1.35	68	326	669	21.79	1.24	127	542	114	21.69	1.24	185	654	35	19.71	0.79
10	59	112	20.00	1.81	69	326	785	21.98	1.32	128	544	688	21.03	1.43	186	657	140	21.35	2.80
11	60	582	21.46	1.56	70	327	685	20.04	1.57	129	550	96	21.43	1.29	187	658	594	21.77	1.15
12	63	37	21.61	1.26	71	334	599	21.56	1.25	130	550	571	21.81	0.77	188	660	334	21.82	1.21
13	66	498	21.98	1.65	72	334	628	21.32	1.38	131	551	49	21.21	1.28	189	660	514	21.01	1.39
14	66	612	21.89	1.09	73	343	720	19.30	1.20	132	556	29	21.16	2.33	190	661	496	19.00	2.48
15	67	515	21.48	1.56	74	345	748	21.85	1.36	133	556	107	21.27	1.17	191	663	97	21.19	1.41
16	72	638	20.17	1.59	75	346	737	21.45	1.22	134	559	67	18.75	1.22	192	663	255	21.50	1.12
17	82	628	19.73	1.00	76	355	695	20.45	1.75	135	561	91	20.75	1.26	193	664	158	19.57	2.07
18	86	46	21.19	1.37	77	356	619	20.70	1.50	136	561	673	21.83	1.07	194	665	595	20.52	1.63
19	94	731	19.02	1.72	78	359	662	20.96	1.24	137	562	449	21.76	1.09	195	667	615	21.34	1.15
20	102	58	21.82	1.08	79	371	780	21.78	1.97	138	563	85	21.91	1.38	196	674	606	20.65	1.55
21	108	40	21.45	1.87	80	376	606	21.53	1.42	139	564	707	21.99	0.99	197	675	172	20.90	1.37
22	109	47	21.68	1.17	81	384	663	21.44	1.36	140	570	444	21.15	1.38	198	675	333	20.95	1.39
23	115	554	21.17	1.27	82	384	702	21.42	1.42	141	574	437	21.29	1.39	199	677	291	21.53	1.27
24	115	705	19.43	1.47	83	387	734	20.89	1.37	142	574	662	21.71	0.96	200	680	604	21.23	1.25
25	118	621	20.68	1.08	84	418	784	21.91	1.93	143	582	440	21.92	1.25	201	681	246	21.70	1.06
26	127	662	21.40	1.19	85	422	593	18.15	2.49	144	585	80	21.43	1.36	202	681	575	21.69	0.76
27	140	671	21.17	1.60	86	422	621	21.98	1.44	145	585	430	21.81	1.05	203	684	255	21.99	1.08
28	142	686	21.93	1.47	87	428	606	21.91	1.27	146	586	422	21.39	1.33	204	686	297	20.58	2.40
29	147	669	20.78	1.30	88	434	681	21.78	1.56	147	588	47	21.52	1.06	205	687	72	21.61	1.21
30	152	767	21.83	1.09	89	434	710	21.09	1.29	148	589	629	21.29	1.39	206	697	547	21.68	1.74
31	153	631	20.55	1.62	90	437	21	21.38	1.22	149	590	604	21.49	1.35	207	699	401	21.81	0.38
32	155	19	19.07	1.73	91	445	666	21.40	1.34	150	596	106	21.77	1.22	208	700	481	21.78	1.67
33	157	737	21.92	1.26	92	447	15	20.75	1.33	151	596	150	21.81	1.15	209	705	489	21.70	2.03
34	160	661	21.95	1.22	93	447	702	21.54	1.31	152	601	431	21.25	1.24	210	706	105	21.95	1.03
35	161	25	21.15	1.75	94	450	591	20.33	1.42	153	602	368	21.45	1.40	211	706	249	21.31	1.32
36	162	618	21.39	1.26	95	452	599	20.74	1.57	154	605	100	19.54	2.22	212	706	268	20.42	2.03
37	164	666	21.62	1.10	96	452	722	21.57	1.15	155	605	440	21.05	1.42	213	706	430	20.88	1.18
38	174	15	18.72	1.68	97	456	651	19.51	1.85	156	605	640	21.92	1.46	214	711	531	21.09	2.19
39	174	629	21.79	1.42	98	462	11	21.24	1.31	157	607	23	18.59	1.20	215	716	345	21.63	1.70
40	178	778	21.71	2.07	99	462	629	20.54	1.49	158	608	295	18.86	2.92	216	720	126	20.96	0.86
41	183	637	20.51	1.80	100	465	615	20.69	1.46	159	609	96	18.81	1.81	217	721	453	21.98	1.66
42	183	717	21.62	1.13	101	468	730	19.97	1.69	160	610	661	20.30	0.87	218	722	266	21.75	1.06
43	193	630	21.42	1.35	102	469	618	21.70	1.08	161	612	372	21.40	1.28	219	725	57	20.46	1.55
44	206	769	20.49	1.54	103	470	739	20.84	1.33	162	613	486	20.26	1.46	220	726	155	21.73	1.18
45	211	653	21.63	1.20	104	472	562	21.71	1.18	163	614	122	21.31	1.19	221	728	128	21.48	2.36
46	215	669	21.40	1.47	105	475	640	21.38	1.32	164	615	317	21.07	1.44	222	728	419	21.93	1.83
47	222	624	21.53	1.20	106	478	48	20.57	1.60	165	616	473	21.51	1.24	223	731	287	20.42	1.53
48	226	716	21.54	1.48	107	479	674	21.53	2.17	166	618	436	21.40	1.33	224	732	504	18.83	1.39
49	228	643	20.04	1.43	108	480	574	20.84	1.41	167	618	496	21.27	1.25	225	738	421	21.53	1.26
50	229	735	21.80	0.84	109	487	51	21.27	1.42	168	618	564	21.62	1.07	226	740	244	21.60	1.37
51	232	626	19.93	1.88	110	488	61	20.39	1.14	169	620	233	21.68	1.13	227	743	493	18.23	2.55
52	236	610	21.27	2.72	111	489	57	21.14	1.46	170	620	672	21.77	2.59	228	744	229	21.36	1.33
53	241	619	21.23	1.28	112	490	45	21.08	1.55	171	628	312	20.74	1.36	229	746	256	21.29	1.89
54	252	750	19.04	1.73	113	492	761	21.91	1.10	172	630	154	20.86	1.10	230	756	350	21.65	1.25
55	258	741	19.96	3.26	114	493	584	21.11	1.20	173	630	216	21.87	1.32	231	757	178	18.52	2.53
56	263	611	20.92	1.45	115	504	19	20.08	2.52	174	631	345	21.81	1.64	232	757	495	21.81	0.93
57	265	677	21.05	1.51	116	506	645	20.79	1.45	175	632	108	19.08	0.99	233	771	148	21.95	1.25
58	276	606	21.12	1.97	117	507	24	21.50	1.20	176	634	336	21.76	1.01	234	775	151	20.57	1.50
59	281	643	21.35	1.62	118	509	34	20.02	1.36										

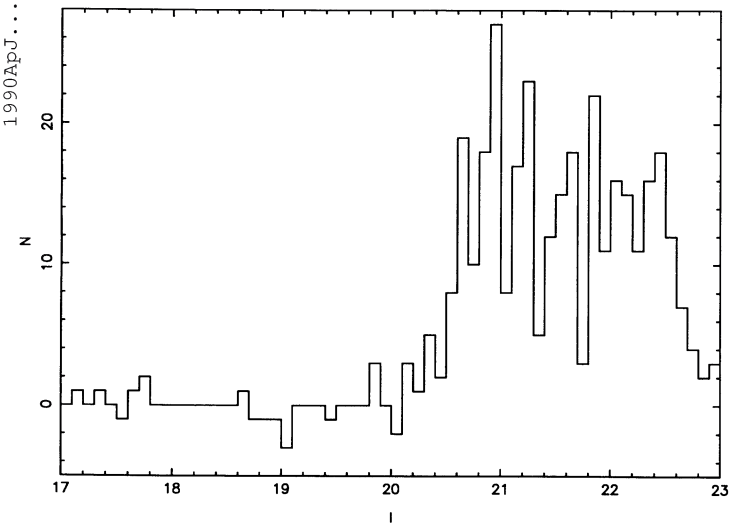

FIG. 7.—I band luminosity function giving the excess in the "dwarf" sample over the "field" sample.

$\langle V-I\rangle = 1.39 \pm 0.03$. The field sample shows a similar distribution with $\langle V-I\rangle = 1.36 \pm 0.05$. Is the dispersion in Figure 8 real? We carried out an additional artificial star experiment adding stars of the appropriate color and magnitude to a 100 × 100 subfield in the center of the galaxy. The experiment yielded $\sigma_{V-I} = 0.13 \pm 0.02$ mag, significantly smaller than $\sigma_{\rm dwarf} = 0.21 \pm 0.02$ and $\sigma_{\rm field} = 0.29 \pm 0.03$ mag. Note that when confusion is the dominant error $\sigma^2_{V-I} < \sigma^2_V + \sigma^2_I$, since the crowding errors at the different wavelengths are well correlated. We infer from this that the color dispersion on the giant branch of Andromeda I is real.

The difference in mean color between the dwarf and field samples in this magnitude interval is not significant. Therefore we are justified in taking $\langle V-I\rangle$ for the dwarf sample as characteristic of And I. After correction for reddening, the mean color of the And I giant branch indicates a mean metallicity [M/H] = -1.4 ± 0.2, a little more metal-rich than the fiducial globular cluster NGC 6752 (Mould, Kristian, and Da Costa 1983). There is a real dispersion in metallicity in And I with over $\frac{2}{3}$ of the stars contained in the range $-2 <$ [M/H] < -1.

Although the dwarf and field samples are statistically the same color at $M_I = -3$, there is a hint of a color gradient in And I, and this is shown in Figure 9. Here the colors of stars with $20 < I < 22$ are shown as a function of radius. A fit to those stars with $V-I < 2$ yields a slope of $2.6 \pm 0.8 \times 10^{-4}$ mag pixel^{-1}, which at this metallicity corresponds approximately to a change of a factor of 5 in heavy element abundance per kiloparsec. Color gradients in dwarf spheroidals have not been seen previously, and this one clearly needs confirmation before we would claim that it is real. In the meantime, however, we can examine the delicacy of this observation as follows. Figure 10 shows the DAOPHOT sky values for all stars in Tables 1 and 2 plotted against radius as defined above. There is a gradient in these sky values of about 1% of sky from center to edge of the V and I frames. This is approximately the level expected for the unresolved background light of And I. The background seems to be a little redder at the edge of the frame than at the center. This corresponds to $\delta(V-I) \approx 0.003$ mag. If we were to "correct" this gradient by adopting a constant background value for the whole frame, we would eliminate (or reverse) the detected color gradient for stars with $I = 22$ (or fainter). However, if the background gradient is mostly unresolved stars, local sky is a valid background determination, and the color gradient is likely to be real.

VI. INTEGRATED LUMINOSITY

Measurement of the luminosity of And I is tricky because the central surface brightness of the galaxy is $\simeq 1\%$ of the night sky. What we have done is to evaluate the luminosity contained within the effective radius and double it. To calculate the effective radius we integrated Figure 2, assuming a background level of 1.05×10^{-3} stars pixel^{-1}. This yield $r_e = 218$ pixels (91″). The average intensity was then calculated within r_e after rejection[1] of all pixels exceeding the maximum brightness

[1] This may be regarded as a masking procedure, where bright stars are almost completely masked out, both from the "object" and "sky" areas.

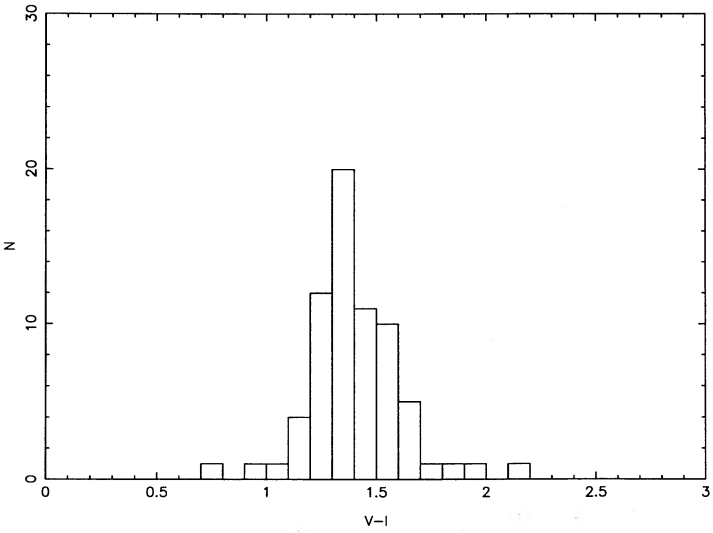

FIG. 8.—The $V-I$ color distribution at $21.45 < I < 21.65$ in the "dwarf" sample. The dispersion is significantly larger than expected from observational errors.

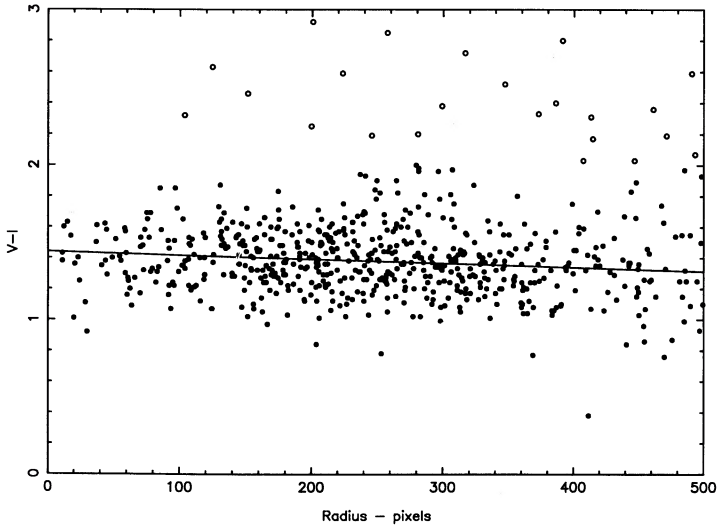

FIG. 9.—The colors of stars with $20 < I < 22$ as a function of radius. The line of best fit has a slope which appears to be different from zero. Stars with $V-I > 2$ (*open circles*) were excluded from this fit.

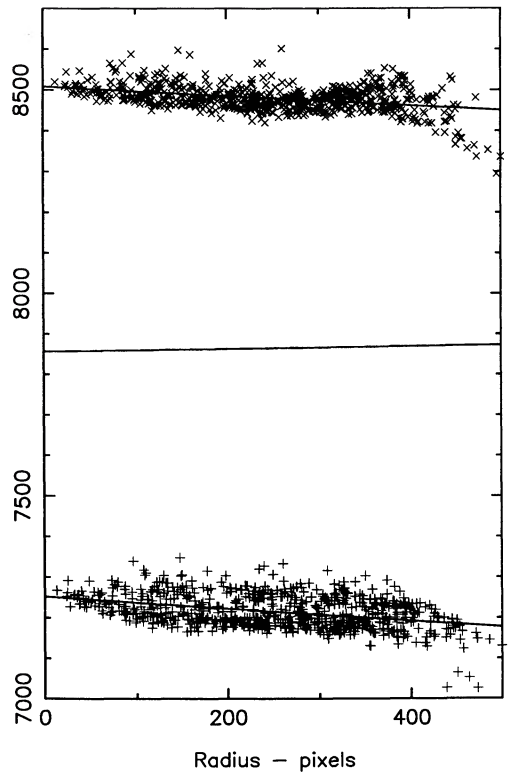

FIG. 10.—The radial distribution of "sky" values for stars in Tables 1 and 2. Values for the I bandpass are indicated with crosses, and values for the V bandpass are indicated with plus signs. The solid lines are the relevant linear regressions. The central line is the difference between the V and I regression lines arbitrarily offset.

expected for stars with $V = 21.5$. A similar calculation was then performed for the on-chip portion of an annulus with radii 400 and 500 pixels. Differencing object and sky, multiplying by the area within r_e, and finally doubling the resultant luminosity, we obtain $V = 13.76$ for And I. From Racine's picture of And I (van den Bergh 1971), we estimate a lower limit on the axial ratio $b/a > 0.7$. The geometrical uncertainty in the correction from effective to total luminosity is thus $+0.0$, -0.2 mag. If we extend our integration of the total light of And I to $r = 400$ pixels, we can reduce this uncertainty, obtaining $V = 13.7 \pm 0.1$.

A second significant uncertainty in the luminosity estimate is caused by background fluctuations due to patchiness in the flat-fielding of the image. The worst "patch" in the image is a $\simeq 0.3\%$ depression in the sky annulus covering $\simeq 100$ pixels in diameter. An upper limit on the resultant uncertainty is obtained by supposing that the image is entirely covered with such low (and high) patches. This upper limit is ± 0.1 mag. The corresponding uncertainty for the I magnitude is ± 0.3 mag, which precludes a useful estimate of the color of And I. The absolute visual luminosity of And I is thus $M_V = -10.9 \pm 0.2$ mag in remarkable agreement with van den Bergh's (1971) original estimate of -11.

This luminosity estimate is consistent with the number of red giant branch tip stars observed in And I. For a simple population of $m = 0.8\ M_\odot$ stars with helium abundance $0.2 < Y < 0.3$, Rood's (1971) models suggest a lifetime over the final magnitude of red giant evolution of between 3.5 and 3.8 Myr. Equation (14) of Renzini and Buzzoni (1986) then predicts 160 ± 16 stars for a population age of 10 Gyr and an initial mass function proportional to $m^{-1.5}$. In Figure 7 there are 150 stars in the range $21.55 < I < 20.55$. The artificial star experiments suggest this count should be increased by $\sim 10\%$ for incompleteness. The agreement is quite satisfactory.

We can also test the assumption that And I is a simple stellar population. Intermediate-age populations exhibit an extended AGB on which a star takes 1.3 Myr to rise a magnitude in luminosity (Renzini 1978). An additional population of stars with an age between 3 and 10 Gyr and a luminosity of, say, 10^5 $L_{V\odot}$ would contribute to the H-R diagram of And I 2.6 stars in the range $20.2 < I < 19.2$. The luminosity functions of the two And I samples contains 4 ± 4 of these stars. The $2\ \sigma$ upper limit on any such population is a contribution of 20% of the total visual luminosity of the galaxy. Similarly, the upper limit on a population of age 0.5 to 3 Gyrs (which would show up as carbon stars[2] with $19.2 < I < 18.2$) is 10%.

VII. CONCLUSIONS

And I is a dwarf spheroidal companion to M31 of a size comparable with the Milky Way's Sculptor dwarf spheroidal. The distance of And I is 790 ± 60 kpc, the absolute magnitude $M_V = -10.9 \pm 0.2$ (cf. -11.1 for Sculptor; Armandroff and Da Costa 1986), and the effective radius is 0.36 kpc (cf. 0.43 for Sculptor; Eskridge 1988). The color of the giant branch implies a mean metallicity $[M/H] = -1.4 \pm 0.2$, higher than that of Sculptor (-1.9 ± 0.2; Kunkel and Demers 1977). This value is also almost $2\ \sigma$ higher than the mean metallicity of Galactic dwarf spheroidals of this luminosity (see Da Costa 1988). We should examine the other Andromeda dwarf spheroidals before commenting on the significance of this result. And I has a detectable spread in metallicity, a common property of all dwarf spheroidals. In Sculptor the presence of carbon stars led Aaronson and Mould (1985) to claim that 5% of the integrated light came from an intermediate-age population (between 1 and 10 Gyr old). In And I the upper limit on such a population is 20%. There is marginal evidence for a color gradient in And I.

We thank Gary Da Costa for helpful suggestions and a careful reading of the manuscript. This work was partially supported by NSF grant 87-21705.

[2] Carbon stars have been found in And II by (Aaronson *et al.* 1985). Spectra have also been obtained of two of the reddest stars in And I. These were of too low S/N to permit classification.

REFERENCES

Aaronson, M., Gordon, G., Mould, J., Olszewski, E., and Suntzeff, N. 1985, *Ap. J. (Letters)*, **296**, L7.
Aaronson, M., and Mould, J. 1985, *Ap. J.*, **290**, 191.
Armandroff, T., and Da Costa, G. 1986, *A.J.*, **92**, 777.
Burstein, D., and Heiles, C. 1982, *A.J.*, **87**, 1165.
Da Costa, G. 1988, in *The Harlow Shapley Symposium on Globular Cluster Systems in Galaxies*, ed. J. Grindlay and A. G. Davis Philip (Dordrecht: Reidel), p. 217.
Eskridge, P. 1988, *A.J.*, **95**, 1706.
Frogel, J., and Elias, J. 1988, *Ap. J.*, **324**, 823.
Frogel, J., Cohen, J., and Persson, S. E. 1983, *Ap. J.*, **275**, 773.
Kunkel, W., and Demers, S. 1977, *Ap. J.*, **214**, 21.
Mateo, M., and Nemec, J. 1989, private communication.
Mighell, K. 1989, *Astr. Ap.*, in press.
Mould, J. 1986, in *Stellar Populations*, ed. C. Norman and M. Tosi (Cambridge: Cambridge University Press), p. 9.

Mould, J., and Aaronson, M. 1983, *Ap. J.*, **273**, 530.
Mould, J., and Kristian, J. 1986, *Ap. J.*, **305**, 591 (MK86).
Mould, J., Kristian, J., and Da Costa, G. 1983, *Ap. J.*, **270**, 471.
———. 1984, *Ap. J.*, **278**, 575.
Renzini, A., and Buzzoni, A. 1986, in *Spectral Evolution of Galaxies*, ed. C. Choisi and A. Renzini (Dordrecht: Reidel), p. 195.
Renzini, A. 1978, in *Advanced Stages of Stellar Evolution*, ed. I. Iben and A. Renzini (Geneva: Geneva Observatory), p. 149.
Rood, H. 1971, *Ap. J.*, **177**, 681.
Stetson, P. 1987, *Pub. A.S.P.*, **99**, 191.
van den Bergh, S. 1971, *Ap. J.* (*Letters*), **171**, L31.

JEROME KRISTIAN: The Observatories of the Carnegie Institution of Washington, 813 Santa Barbara Street, Pasadena, CA 91101-1291

JEREMY MOULD: 105-24, Division of Physics, Mathematics, and Astronomy, California Institute of Technology, Pasadena, CA 91125